Analog of the electromagnetically-induced-transparency effect for two nanomechanical or micromechanical resonators coupled to a spin ensemble

Yue Chang (常越) and C. P. Sun (孙昌璞)*
Institute of Theoretical Physics, The Chinese Academy of Sciences, Beijing, 100080, China
(Received 20 January 2011; published 24 May 2011)

We study a hybrid nanomechanical system coupled to a spin ensemble as a quantum simulator to favor a quantum interference effect, electromagnetically induced transparency (EIT). This system consists of two nanomechanical resonators (NAMRs), each of which is coupled to a nuclear spin ensemble, and can be regarded as a crucial element in the quantum network of NAMR arrays coupled to spin ensembles. Here, the nuclear spin ensembles behave as a long-lived transducer to store and transfer the NAMRs' quantum information. This system shows the analog of the EIT effect under the driving of a probe microwave field. The double EIT phenomenon emerges in the large-N (the number of nuclei) limit within the low excitation approximation, because the interactions between the spin ensemble and the two NAMRs are reduced to the coupling of three harmonic oscillators. Furthermore, the group velocity is reduced in the two absorption windows.

DOI: 10.1103/PhysRevA.83.053834 PACS number(s): 42.50.Gy, 73.21.La, 03.67.−a

I. INTRODUCTION

In quantum information studies, an important task is the long-lived storage and remote quantum state transfer [1–5] of quantum information. There exist several approaches to the implementation of quantum storage, such as electromagnetically induced transparency (EIT) based on a three-level atomic ensemble [6–14], nuclear spins coupled to electrons [15], and polarized molecular ensembles coupled to cavity fields in superconducting transmission lines [16–18]. A nuclear spin ensemble has the advantage that its transverse relaxation time T_2 can reach a time scale of a second [19,20]. In earlier works [15,19,21,22], nuclei ensembles have been used to store the quantum information of electron spins, since the electron spin's decoherence time T_{e2} is in the order of 10 ms [20,23], which is much shorter than the nuclear spin relaxation time.

Recently, optomechanical systems containing nanomechanical or micromechanical resonators have inspired extensive studies in many aspects, such as the entanglements of the mechanical resonators with light [24–27], and even atoms [28–30], cooling mechanical resonators through light pressure [31–35], and nonclassical states in hybrid systems [36–38]. In fact, the nanomechanical and micromechanical resonator's decoherence time T_{r2} is shorter [39,40] ($\sim$100 μs) than the lifetime of the nuclear spins. Therefore, it is expected to store the information of the nanomechanical or micromechanical resonator in the nuclear spins. Actually, the coupling between the nuclear spin ensemble (or a single spin) and the mechanical resonator tips has drawn much attention [41–48], both in theory and in experiments. An important innovation based on the coupling of single or few spins to the mechanical tip is magnetic resonance force microscopy (MRFM) [41–47,49]. MRFM uses a cantilever tipped with a ferromagnetic particle, producing an inhomogeneous magnetic field that couples the mechanical tip to the sample spins. By measuring the displacement of the tip with an interferometer, a series of two-dimensional images of the spin sample is acquired [50]. In practice, the spin sample is usually a spin ensemble containing a lot of electrons or nuclear spins, which could be excited to show the collective behavior. Such collective motion could achieve effective strong coupling to the nanomechanical resonator (NAMR).

With the above mentioned investigations about various hybrid systems concerning nuclear spin ensembles and NAMRs, Rabl *et al.* [51] explored the possibility of using the short-lifetime NAMR as a quantum data bus for spin qubits coupled to magnetized mechanical tips, and the mechanical resonators are coupled through Coulomb forces. This study motivates us to utilize the nuclear spin ensemble itself as a long-lived data bus (the spin ensemble also behaves as a quantum transducer [52]) to realize effective couplings among the NAMRs. The advantage of our proposal is that the quantum transducer has a lifetime much longer than the NAMR's. Our setup is shown in Fig. 1, where an array of NAMRs is coupled to nuclear spin ensembles, which are placed between the nearest two tips. Each spin ensemble induces interaction between the corresponding tips, and the quantum information of the tips can be transferred from one to the another one by one. This dynamic process realizing quantum information transfer physically depends on an controllable coupling among the three systems, two NAMRs and a spin ensemble. We will show that the double EIT effect exists in our present setup and plays an important role in the coherent storage of quantum information in this hybrid-element subsystem.

In the conventional EIT effect based on a Λ-type three-level atomic ensemble on a two-photon resonance, a driving light suppresses the absorption of another light (the probe light), and even makes the probe light transparent at the frequency at which the probe light should be absorbed strongly without the driving field [53]. An important physical mechanism in this EIT effect is that the pump light induces an ac Stark splitting of the excited state. As a result, the probe light is off-resonant with the energy spacing of the energy levels to which it couples. Actually, the EIT effect analog exists in a system of two coupled harmonic oscillators, one of which is subject to a harmonic driving force [54] . In fact, the coupling between the two harmonic oscillators will change their original frequencies and make the absorbed power deviate from resonance. This

*suncp@itp.ac.cn; http://www.itp.ac.cn/∼suncp

 ©2011 American Physical Society

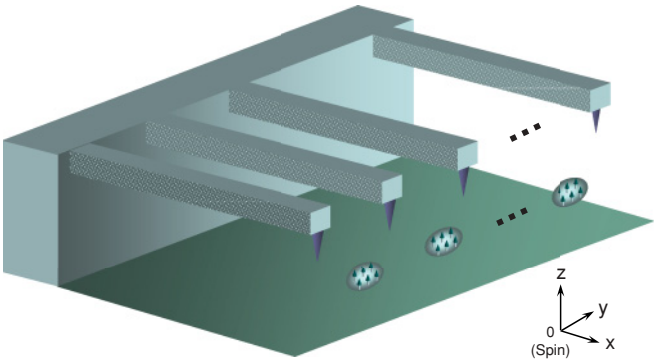

FIG. 1. (Color online) Schematic setup of the NAMR–spin ensemble–NAMR–. . . system. Here, the spin ensembles are placed between two nearest NAMRs in the NAMR array, and each NAMR has a tiny ferromagnetic particle in the mechanical tip. The spin ensembles behave as a transducer that stores the NAMRs' quantum information and transfers them from one NAMR to the next one.

reason is similar to that in the conventional EIT phenomenon. We show that our proposed setup consisting of a magnetized mechanical tip coupled to a nuclear ensemble, which behaves as a two-coupled-harmonic-oscillator system, can also exhibit a phenomenon similar to the EIT effect in the system with light-atom interaction.

We will study in detail the double EIT effect analog in a subnetwork of the whole structure shown in Fig. 1, a NAMR–spin ensemble–NAMR coupling system. In the low-excitation limit with large-N (the number of nuclear spins) limit, the spin excitation behaves as a single-mode boson [14,15,29] coupled, respectively, to the two mechanical tips. In this case, the interaction between the spins and each tip is the coupling between two harmonic oscillators with an effective amplified strength proportional to $\sqrt{N}$. In general, this three-oscillator coupling system has three eigenfrequencies (taking account of the degeneracy). And we show that there are two absorption windows for the probe microwave field, with the absorption peaks corresponding to the three eigenfrequencies. In these two windows with normal dispersion relations, the group velocity of the microwave field is reduced dramatically. These transparency and slow-light phenomena correspond to the EIT effect.

The paper is organized as follows: In Sec. II, we illustrate the subnetwork composed of two nanomechanical resonators coupled to a spin ensemble. In Sec. III, we study the mechanical analog of the EIT effect in a NAMR–nuclear ensemble coupling system, and we make a comparison with the atomic, molecular, and optical (AMO) system by revisiting the conventional EIT phenomenon. In Sec. IV, we study the double EIT effect in the subnetwork hybrid system, and we show the slowing light phenomenon in Sec. V. In Sec. VI, we summarize our result.

II. SETUP AND MODELING FOR THE QUANTUM TRANSDUCER

We now consider a hybrid system consisting of two NAMRs and a nuclear spin ensemble containing N spins. This system is the basic unit for constructing the whole quantum network (Fig. 1). The spin-NAMR hybrid system is illustrated in Fig. 2.

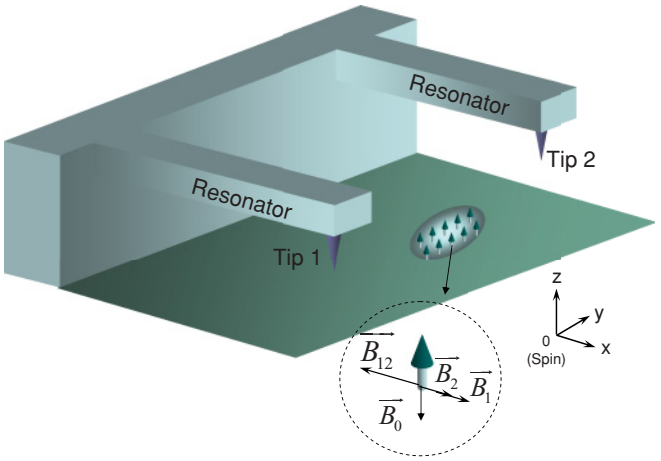

FIG. 2. (Color online) Schematic setup of the NAMR–spin ensemble–NAMR coupling system. The ensemble of spins is placed between two NAMRs, each of which has a tiny ferromagnetic particle in the tip. The directions of the two magnetic fields produced by the two tips are both along the x axis. The origin of the coordinate frame is at the center of the spin ensemble. The spin ensemble is also exposed in two static magnetic fields, $\vec{B}_{12}$ along the x axis and $\vec{B}_0$ along the z axis.

In this setup, each NAMR is coupled to the ensemble of N 1/2-spin particles by a tiny ferromagnetic particle attached to it. The origin of the reference frame is chosen to be the center of the nuclear spin ensemble. The NAMRs can oscillate in the z direction, and each magnetized tip attached to the corresponding NAMR produces a dipolar magnetic field at the position of the spins as [55]

$$\vec{B}_j = \frac{\mu_0[3(\vec{m}_j\cdot\vec{n}_j)\vec{n}_j - \vec{m}_j]}{4\pi r_j^3}, \quad j = 1,2, \tag{1}$$

where μ_0 is the vacuum magnetic conductance, $\vec{m}_j$ is the jth ferromagnetic particle's magnetic moment, and $\vec{n}_j$ is the corresponding unit vector pointing in the direction from the tip to the spin. Here, r_j, which varies due to the oscillation of the NAMR along the z direction, is the distance between the magnetic tip and the spin. In our setup, both of the magnetic moments in the two tips are in the x direction as $\vec{m}_1 = m_1\hat{e}_x$ and $\vec{m}_2 = m_2\hat{e}_x$. The equilibrium positions of the two NAMRs are $\vec{r}_1$ and $\vec{r}_2$, respectively, and both $\vec{r}_1$ and $\vec{r}_2$ are in the yz plane. We have assumed that the spins are confined in a very small volume, and the magnetic fields produced by the two ferromagnetic particles at the spin ensemble are uniform as $\vec{B}_1 = (B_1(z_1),0,0)$ and $\vec{B}_2 = (B_2(z_2),0,0)$, respectively, where

$$B_j(z_j) \approx A_j - G_j z_j, \quad j = 1,2, \tag{2}$$

with $z_1(z_2)$ the small deviation of tip 1 (tip 2) from the equilibrium position. Here, $A_1 = -\mu_0 m_1/(4\pi|\vec{r}_1|^3)$, $A_2 = -\mu_0 m_2/(4\pi|\vec{r}_2|^3)$, and the magnetic field gradients are

$$G_1 = \frac{3r_{1z}\mu_0 m_2}{4\pi|\vec{r}_1|^5}, \quad G_2 = \frac{3r_{2z}\mu_0 m_2}{4\pi|\vec{r}_2|^5}, \tag{3}$$

where $r_{jz} = \vec{r}_j\cdot\hat{e}_z$, for $j = 1,2$. Besides these two magnetic fields, the spins are also exposed to two static magnetic fields, $\vec{B}_{12} = (-A_1 - A_2,0,0)$ and $\vec{B}_0 = -B_0\hat{e}_z$. We note that in experiments [43,44,56], the distance between the magnetized

tip and the nuclear ensemble is on the order of 100 nm, and the nuclear spin ensemble containing more than 100 nuclei is attached in a quantum dot with a diameter on the order of 10 nm. Thus the the magnetic field $B_j(z_j)$ is approximately homogeneous in the nuclear ensemble when z_j is fixed.

Both of the NAMRs are described as harmonic oscillators with effective masses M_j and frequencies ω_j. Then the Hamiltonian H_0^d of this spin-NAMRs coupling system is

$$H_0^d = \frac{p_1^2}{2M_1} + \frac{p_2^2}{2M_2} + \frac{1}{2}M_1\omega_1^2 z_1^2 + \frac{1}{2}M_2\omega_2^2 z_2^2 + \sum_{j=1}^{N}\left(g_1\sigma_j^x z_1 + g_2\sigma_j^x z_2 + g_0\sigma_j^z\right), \quad (4)$$

where p_j is the momentum of the NAMR j, and σ_x and σ_y are Pauli matrices describing the spin. Here, the spin-NAMR coupling strength is $g_j = g_s\mu_B G_j/2$ for $j = 1,2$, where g_s is the g factor of the spin, μ_B is the Bohr magneton, and $g_0 = g_s\mu_B B_0/2$. Note that to first order, the magnetic dipole interaction

$$H_{d-d} = \frac{\mu_0[3(\vec{m}_1\cdot\hat{e}_{12})(\vec{m}_2\cdot\hat{e}_{12}) - \vec{m}_1\cdot\vec{m}_2]}{4\pi|\vec{r}_1 - \vec{r}_2|^3}, \quad (5)$$

where $\hat{e}_{12}$ is the unit vector pointing in the direction from tip 1 to tip 2, vanishes in our model.

To see the analog of the EIT effect, we apply a probe microwave field $\vec{B}_p = -\hat{e}_x B_p\cos\Omega t$ coupled to the spin ensemble. This coupling is described by the interacting Hamiltonian

$$H_I = \frac{1}{2}g_s\mu_B B_p\cos\Omega t\sum_{j=1}^{N}\sigma_j^x. \quad (6)$$

The probe alternating magnetic field is similar to the probe light in the Λ-type atomic ensemble. The total Hamiltonian $H^d = H_0^d + H_I$ depicts the subnetwork illustrated in Fig. 2.

When N is large and with low excitations of the spins, the excitations of the spins are described by two bosonic operators [14,15,29],

$$b = \frac{1}{\sqrt{N}}\sum_{j=1}^{N}\sigma_j^- \quad (7)$$

and its conjugate $b^\dagger$, where the commutation relation between b and $b^\dagger$ is

$$[b,b^\dagger] \approx 1. \quad (8)$$

In terms of b and $b^\dagger$ defined above, the Hamiltonian in Eq. (4) is rewritten as

$$H_0^d = \frac{\hbar\omega_1}{2}\left(P_1^2 + Z_1^2\right) + \frac{\hbar\omega_2}{2}\left(P_2^2 + Z_2^2\right) + \frac{\hbar\omega_0}{2}\left(P_0^2 + Z_0^2\right) + \hbar\sqrt{N}\sum_{j=1}^{2}G_j Z_0 Z_j. \quad (9)$$

Here, we have defined the dimensionless operators

$$Z_0 = \frac{b + b^\dagger}{\sqrt{2}}, \quad P_0 = i\frac{b^\dagger - b}{\sqrt{2}}, \quad (10)$$

$$Z_j = \sqrt{\frac{M_j\omega_j}{\hbar}}z_j, \quad P_j = \frac{p_j}{\sqrt{\hbar M_j\omega_j}}, \quad j = 1,2. \quad (11)$$

The coupling constants are $G_j = g_j\sqrt{2\hbar/M_j\omega_j}/\hbar$, for $j = 1,2$, and $\omega_0 = 2g_0/\hbar$. In experiments, the parameters ω_j ($j = 1,2$) and ω_0 are on the order of 10^6 Hz, and $G_j$can reach the order of 10^5 Hz.

Before pursuing further investigations of the double EIT effect in this hybrid system, we would like to show the mechanical analog of the EIT phenomenon in a NAMR–spin ensemble coupling system with only a single NAMR, as the basic physics in the double EIT phenomenon depends on the coherent coupling of the NAMR to the nuclear spin ensemble.

III. MECHANICAL ANALOG OF EIT

In this section, we show the analog of the EIT effect in the single NAMR coupled to a spin ensemble system. To this end, we will compare it with the EIT phenomenon in the AMO system.

To reveal the basic physical mechanism, we first consider a system consisting of a NAMR and a nuclear spin ensemble containing N spins. The spin-NAMR hybrid system is illustrated in Fig. 3(a). The origin of the reference frame is chosen to be the center of the nuclear spin ensemble. The NAMR can oscillate along the z direction, and the magnetized tip attached to the NAMR produces a dipolar magnetic field at the position of the spin, with magnetic field $\vec{B} = (B(z),0,0)$, where

$$B(z) \approx A - Gz, \quad (12)$$

with $A = -\mu_0 m/(4\pi|\vec{r}|^3)$, and the magnetic field gradient is $G = 3r_z\mu_0 m/(4\pi|\vec{r}|^5)$. Here, $\vec{m} = m\hat{e}_x$ is the ferromagnetic particle's magnetic moment, $\vec{n}$ is the unit vector pointing in the direction from the tip to the spin, and $\vec{r}$ in the yz plane is the equilibrium position of the tip. We assume that the spins are confined in a very small volume. In the gradient G, $r_z = \vec{r}\cdot\hat{e}_z$.

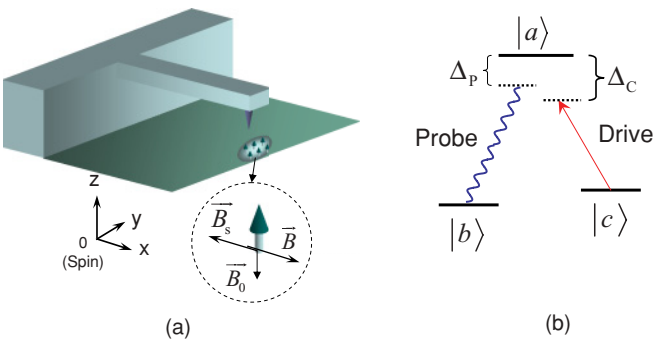

FIG. 3. (Color online) Schematic of a NAMR couple to a spin ensemble (a) and a Λ-type three-level atom (b). The EIT effect base on the atomic ensemble (b) where each atom is coupled to a driving light and probe light has a analog in the two-harmonic-oscillator coupling system derived from the structure (a). In (a), the spin ensemble is placed under the NAMR, which has a tiny ferromagnetic particle in the tip. The direction of the magnetic field produced by the magnetized tip is along the x axis. The origin of the coordinate frame is at the center of the spin ensemble. The spin ensemble is also exposed to two static magnetic fields, $\vec{B}_s$ along the x axis and $\vec{B}_0$ along the z axis.

Besides the magnetic field $B(z)$ produced by the magnetized tip, the spins are also exposed to two static magnetic fields, $\vec{B}_s = (-A,0,0)$ and $\vec{B}_0$.

The magnetized tip is described as a harmonic oscillator with the effective mass M and frequency ω. With a probe microwave field $\vec{B}_\mathrm{p} = -\hat{e}_x B_\mathrm{p} \cos \Omega t$, the Hamiltonian H of this spin-NAMR hybrid system is $H = H_0 + H_I$, where

$$H_0 = \frac{p^2}{2M} + \frac{1}{2}m\omega^2 z^2 + \sum_{j=1}^{N}\left(g\sigma_j^x z + g_0\sigma_j^z\right), \tag{13}$$

with p the momentum of the NAMR. Here, the spin-NAMR coupling strength $g = g_s\mu_B G/2$.

Actually, when N is large and with low excitations of the spins, following a similar procedure to that in the last section, the Hamiltonian in Eq. (13) is rewritten as

$$H_0 = \frac{\hbar\omega_0}{2}\left(P_0^2 + Z_0^2\right) + \frac{\hbar\omega}{2}(P^2 + Z^2) + \hbar G\sqrt{N}Z_0 Z, \tag{14}$$

where

$$Z = \sqrt{\frac{M\omega}{\hbar}}z, \quad P = \frac{p}{\sqrt{\hbar M\omega}}, \tag{15}$$

and the NAMR–spin ensemble coupling constant is $G = g\sqrt{2\hbar/m\omega}/\hbar$.

Equation (14) shows that under the low-excitation approximation with the large-N limit, the NAMR–spin ensemble coupling system is described by a two-harmonic coupling system if $\omega_0 > 0$, with the coupling constant proportional to $\sqrt{N}$. In the large-N limit with low excitations, H_I is written as

$$H_I = \hbar\sqrt{N}G_\mathrm{p}Z_0(e^{-i\Omega t} + e^{i\Omega t}), \tag{16}$$

where $G_\mathrm{p} = g_s\mu_B B_\mathrm{p}/(\sqrt{2}\hbar)$. The set of Heisenberg-Langevin equations gives

$$\begin{aligned}\partial_t^2 Z_0 = &-\gamma_0\dot{Z}_0 - \omega_0^2 Z_0 - \omega_0\sqrt{N}GZ \\ &- \omega_0\sqrt{N}G_\mathrm{p}(e^{-i\Omega t} + e^{-i\Omega t}),\end{aligned} \tag{17}$$

$$\partial_t^2 Z = -\gamma\dot{Z} - \omega^2 Z - \omega\sqrt{N}GZ_0, \tag{18}$$

where γ_0 (γ) is the decay rate for Z_0 (Z). The probe microwave field also provides a "driving" term in the set of equations (17) and (18), just as the probe light behaves in the conventional EIT phenomenon. Here, we have ignored the fluctuations as we are interested in the steady states and the fluctuations' expectation values about the steady states are zero. The solutions to Eqs. (17) and (18) have the form

$$Z_{0s}(t) = Z_{0s}(\Omega)e^{-i\Omega t} + Z_{0s}(-\Omega)e^{i\Omega t} \tag{19}$$

and

$$Z_s(t) = Z_s(\Omega)e^{-i\Omega t} + Z_s(-\Omega)e^{i\Omega t}. \tag{20}$$

It follows from Eqs. (17)–(20) that the solution for $Z_{0s}(\Omega)$ is

$$Z_0(\Omega) = \frac{\omega_0\sqrt{N}G_\mathrm{p}\xi}{-N\omega_0\omega G^2 + \xi_0\xi}, \tag{21}$$

where

$$\xi_0 = i\Omega\gamma_0 - \omega_0^2 + \Omega^2 \tag{22}$$

and

$$\xi = i\Omega\gamma - \omega^2 + \Omega^2. \tag{23}$$

The magnetic susceptibility of the alternating magnetic field $\vec{B}_\mathrm{p}$ is

$$\chi_M = \frac{\vec{M}}{\vec{B}_\mathrm{p}/\mu_0 - \vec{M}} \approx \frac{\mu_0\vec{M}}{\vec{B}_\mathrm{p}}, \tag{24}$$

where μ_0 is the permeability of vacuum, and the magnetization intensity $\vec{M}$ is

$$\begin{aligned}\vec{M} &= \hat{e}_x\frac{g_s\mu_B}{2}\left\langle\sum_{j=1}^{N}\sigma_j^x\right\rangle/V \\ &= \hat{e}_x\frac{\sqrt{N}g_s\mu_B}{\sqrt{2}V}[Z_{0s}(\Omega)e^{-i\Omega t} + \text{c.c.}],\end{aligned} \tag{25}$$

with the volume of the spin ensemble V. Here, we have assumed that the magnetization intensity $|\vec{M}|$ is small compared with $|\vec{B}_\mathrm{p}|/\mu_0$, in order to ensure the validity of the expansion in Eq. (24). Consequently, the magnetic susceptibility $\chi_M(\Omega)$ is

$$\chi_M(\Omega) = -\frac{\mu_0 g_s\mu_B}{\sqrt{2}V B_\mathrm{p}}\sqrt{N}Z_{0s}(\Omega). \tag{26}$$

The real and imaginary parts of $\chi_M(\Omega)$ depict the dispersive response and the absorption, respectively. With the parameters as (in units of ω_0) $\omega = 1$, $\gamma_0 = 5\times10^{-2}$, $\gamma = 10^{-7}$, $G_\mathrm{p} = 1$, $N = 20$, $B_\mathrm{p} = \sqrt{2}\hbar G_\mathrm{p}/g_s\mu_B$, and $V = (4\pi/3)10^3$ nm^3, we plot Re$[\chi_M(\Omega)]$ and Im$[\chi_M(\Omega)]$ in Figs. 4(a) and 4(b), for $G = 0$ and $G = 0.05$, respectively. In Fig. 4(a), the absorbed peak is at the frequency $\Omega = \omega$, as the nuclear spin ensemble is decoupled with the NAMR. The absorption window and slow-light phenomenon for the microwave field due to the coupling with the NAMR are illustrated in Fig. 4(b), which shows the analog of EIT. We note that there are two absorption peaks in Fig. 4(b), corresponding approximately to the two eigenfrequencies derived from Eq. (14). In the absorption window, the slope of Re$[\chi_M(\Omega)]$ is positive, which illustrates that the group velocity of the microwave field is reduced dramatically.

To see why the above mechanical system can display an EIT analog and its intrinsic mechanism in detail, we revisit the EIT effect in an AMO system shown in Fig. 3(b). Figure 3(b) shows the energy levels of the Λ-type atom of the atomic ensemble. Here, the single-mode driving field makes a transition between the excited state $|a\rangle$ and the second lowest state $|c\rangle$ with the

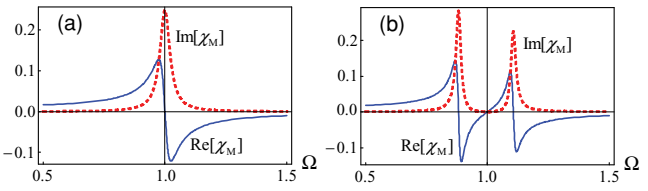

FIG. 4. (Color online) The frequency dependence of the real part (the blue solid line) and the imaginary part (the red dashed line) of the susceptibility $\chi_M(\Omega)$ in a single NARM-spin ensemble coupling system. The NAMR-spin coupling constant is (a) $G = 0$ and (b) $G = 0.05$. When NAMR-spin coupling exists, there is a window in the absorption spectrum, with a positive slope of Re$[\chi_M(\Omega)]$ in the window. This is an analog of the EIT effect in the atomic ensemble.

detuning $\Delta_c = \omega_{ac} - \nu_c$, while the single-mode probe light makes a transition between the state $|a\rangle$ and the lowest state $|c\rangle$ with the detuning $\Delta_p = \omega_{ab} - \nu_p$. Here, ω_{ac} (ω_{ab}) is the energy level spacing between the states $|a\rangle$ and $|c\rangle$ ($|b\rangle$), and ν_c (ν_p) is the frequency of the driving (probe) light. In the rotating frame with respect to [14]

$$\nu_p S + (\omega_{ab} - \omega_{ac}) \sum_{j=1}^{N_a} |c\rangle_{jj}\langle c| + \nu_p a^\dagger a, \tag{27}$$

in the large-N_a (the number of atoms) limit with low excitations of the atom ensemble, the Hamiltonian is

$$H_{EIT} = \Delta_p A^\dagger A + (g_p\sqrt{N_a} a A^\dagger + g_c e^{i(\Delta_c - \Delta_p)t} A^\dagger C + \text{H.c.}), \tag{28}$$

where the atomic collective excitations are described by

$$A^\dagger = \frac{1}{\sqrt{N_a}} \sum_{j=1}^{N_a} |a\rangle_{jj}\langle b|, \quad C = \frac{1}{\sqrt{N_a}} \sum_{j=1}^{N_a} |b\rangle_{jj}\langle c|, \tag{29}$$

and the operators defined in Eqs. (29) satisfy the commutation relations approximately as [14] $[A, A^\dagger] \approx 1$, $[C, A^\dagger] \approx 0$, and $[C, C^\dagger] \approx 1$. Here, a ($a^\dagger$) is the annihilation (creation) operator of the probe light, and $|\alpha\rangle_{jj}\langle\beta|$ ($\alpha, \beta = a,b,c$) is jth atom's flip operator. g_p (g_c) is the coupling constant of the probe (driving) light and a single atom with the corresponding energy levels. We assume that both g_p and g_c are real. As shown in Eq. (28) the EIT effect based on the Λ-type three-level atomic ensemble can be reexplained by the coupling of two "harmonic oscillators" (depicted by the collective excitation operators A and C), with coupling strength g_c. Here, the coupling of the A mode to the quantized field of a can compare with the semiclassical coupling in Eq. (14). Note that under the rotating-wave approximation, the Hamiltonian H in Eqs. (14) and (16) has the same form as H_{EIT} in Eq. (28). As a result, the hybrid system consisting of a NAMR and a nuclear spin ensemble can exhibit the analog of the EIT phenomenon.

IV. DOUBLE EIT ANALOG AND SLOWING LIGHT

We have studied the analog of the EIT effect in the last section for the basic part of our hybrid NAMR-spin coupling network. In this section, we study the double EIT effect in a system consisting of two NAMRs coupled to an N spin ensemble. We first rewrite the Hamiltonian H_0^d as

$$H_0^d = \frac{\hbar\omega_1}{2}\left(P_1^2 + Z_1^2\right) + \frac{\hbar\omega_2}{2}\left(P_2^2 + Z_2^2\right) + \frac{\hbar\omega_0}{2}\left(P_0^2 + Z_0^2\right) + \hbar\sqrt{N}\sum_{j=1}^{2} G_j Z_0 Z_j. \tag{30}$$

Equation (30) shows a coupled-oscillator system, where two harmonic oscillators (NAMRs) couple to another oscillator (spin ensemble) with the coupling constants strengthening by $\sqrt{N}$, respectively. The interaction of the spin ensemble and the probe microwave field is described in Eq. (16).

With the same procedure as used in the last section, the steady-state solution $Z_0^d(\Omega) = \omega_0\sqrt{N}G_p\xi_1\xi_2/D(\Omega)$, where

$$D(\Omega) = -N\omega_0\left(\omega_2 G_2^2\xi_1 - \omega_1 G_1^2\xi_2\right) + \xi_0\xi_1\xi_2 \tag{31}$$

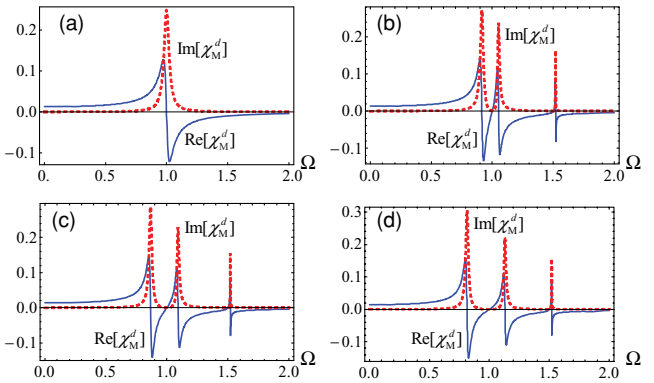

FIG. 5. (Color online) The frequency dependence of the real part (the blue solid line) and the imaginary part (the red dashed line) of the magnetic susceptibility $\chi_M(\Omega)$. The values of G_1 and G_2 are (a) $G_1 = G_2 = 0$, (b) $G_1 = 0.03$ and $G_2 = 0.05$, (c) $G_1 = G_2 = 0.05$, and (d) $G_1 = 0.07$ and $G_2 = 0.05$. When G_1 and G_2 are not zero, the double EIT effect appears with two absorption windows.

and

$$\xi_j = i\Omega\gamma_j - \omega_j^2 + \Omega^2, \quad j = 0,1,2. \tag{32}$$

Here, γ_j ($j = 1,2$) is the decay rate of the jth NAMR.

Consequently, the magnetic susceptibility χ_M^d is

$$\chi_M^d(\Omega) = -\frac{\mu_0 g_s \mu_B}{\sqrt{2}VB_p}\sqrt{N}Z_0^d(\Omega), \tag{33}$$

whose real and imaginary parts depict the dispersive response and the absorption, respectively. We note that, generally, when the decay rates $\gamma_0 \ll \omega_0$, $\gamma_1 \ll \omega_1$, and $\gamma_2 \ll \omega_2$, $D(\Omega)$ is approximately zero with three non-negative real values of Ω, which means that there are three absorbing peaks in $\chi_M^d(\Omega)$. Actually, we can also observe the three absorbed peaks without referring to the steady-state solution $Z_0^d(\Omega)$. From the Hamiltonian (30), the Heisenberg equations follow as

$$\left(-\omega_0^2 + \Omega^2\right)Z_0(0) - \omega_0\sqrt{N}[G_1 Z_1(0) + G_2 Z_2(0)] = \omega_0\sqrt{N}G, \tag{34}$$

$$(-\omega_1^2 + \Omega^2)Z_1(0) - \omega_1\sqrt{N}G_1 Z_0(0) = 0, \tag{35}$$

$$(-\omega_2^2 + \Omega^2)Z_2(0) - \omega_2\sqrt{N}G_2 Z_0(0) = 0. \tag{36}$$

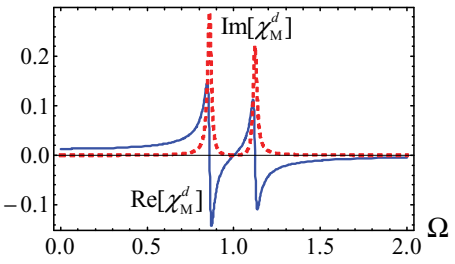

FIG. 6. (Color online) The frequency dependence of the real part (the blue solid line) and the imaginary part (the red dashed line) of the magnetic susceptibility $\chi_M^d(\Omega)$ in the special situation where the two absorption windows are reduced to one.

Obviously, the determinant

$$\det\begin{pmatrix} -\omega_0^2+\Omega^2 & -\omega_0\sqrt{N}G_1 & -\omega_0\sqrt{N}G_2 \\ -\omega_1\sqrt{N}G_1 & -\omega_1^2+\Omega^2 & 0 \\ -\omega_2\sqrt{N}G_2 & 0 & -\omega_2^2+\Omega^2 \end{pmatrix} \quad (37)$$

is just $D(\Omega)$. Thus, the vanishing determinant means the three peaks correspond to the three eigenfrequencies in the Hamiltonian (30). This is the physical mechanism of the mechanical analog of the double EIT effect.

In Figs. 5(a)–5(d), we plot the real and imaginary parts of $\chi_M^d(\Omega)$ versus the microwave field's frequency Ω with different values of G_1 and G_2, while other parameters are fixed as (in units of ω_0) $\omega_1 = 1$, $\omega_2 = 1.5$, $\gamma_0 = 5\times10^{-2}$, $\gamma_1 = \gamma_2 = 10^{-7}$, $G = 1$, $N = 20$, $B = \sqrt{2\hbar G/g_s\mu_B}$, and $V = (4\pi/3)10^3$ nm^3. It is shown in Fig. 5(a) that when the coupling strength $G_1 = G_2 = 0$, the single absorbed peak appears at the frequency ω_0. When we increase G_1 and G_2 , there are three absorbed peaks with two windows, each of which is localized between the nearest two absorption peaks. Figures 5(b)–5(d) illustrate the double EIT effect with three peaks corresponding to three nondegenerate solutions to the equation $D(\Omega) = 0$. We notice that, in some situations, the absorption peaks degenerate to two even if the solutions to $D(\Omega) = 0$ are nondegenerate. For example, when $\omega_1 \approx \omega_2$, which leads to $\xi_1 \approx \xi_2 = \xi$, the magnetic susceptibility $\chi_M^d(\Omega)$ becomes

$$\chi_M^d(\Omega) \approx \frac{N\mu_0 g_s\mu_B\omega_0 G_p\xi}{\sqrt{2}VB_p\left[N\omega_0\left(\omega_2G_2^2-\omega_1G_1^2\right)-\xi_0\xi\right]}. \quad (38)$$

There are only two non-negative roots for the zeros of the dominator on the right-hand side of Eq. (38), corresponding to two resonant peaks in the absorbing spectrum. This situation is illustrated in Fig. 6, with the same parameters as that in Fig. 5(b), except for the NAMRs' frequencies $\omega_1 = \omega_2 = 1$.

Finally, to witness the existence of the double EIT phenomenon in our setup, we consider the velocity of signal transfer as follows. The group velocity of the alternating magnetic field propagating in the spin ensemble is defined as [14]

$$v_g = \mathrm{Re}\left[\frac{d\Omega}{d[\Omega n(\Omega)/c]}\right] = \mathrm{Re}\left[\frac{c}{n(\Omega)+\Omega\partial_\Omega n(\Omega)}\right], \quad (39)$$

where $n(\Omega)$ is the complex refractive index defined as

$$n(\Omega) = \sqrt{1+\chi_M(\Omega)}, \quad (40)$$

and c is the velocity of light in vacuum. The group velocity (in units of the light velocity $c = 1/\sqrt{\varepsilon_0\mu_0}$ in vacuum) in the frequency region between the first and last two absorbed peaks is illustrated in Fig. 7(a) and 7(b), respectively, with the parameters the same as in Fig. 5(b). It is shown in Fig. 7 that in both of the two absorption windows, the group velocity of the microwave field is reduced dramatically. It is indeed similar to that in the atomic EIT effect.

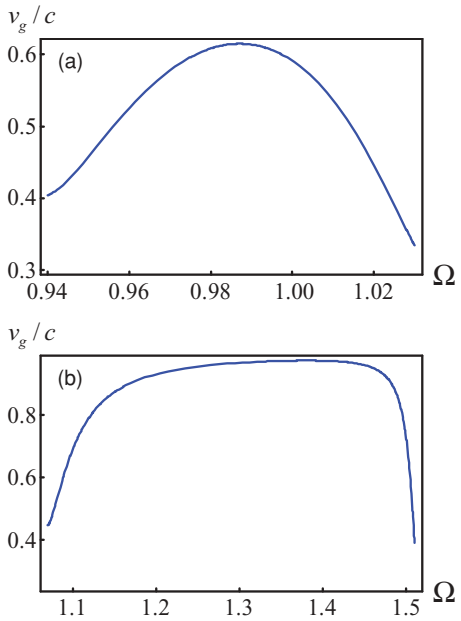

FIG. 7. (Color online) The group velocity v_g in the frequency region between the first two (a) and the last two (b) absorbed peaks in Fig. 5(b). The microwave field's group velocity is reduced dramatically in both of these two windows.

V. SUMMARY

We have proposed and studied a hybrid setup where two NAMRs are coupled to a nuclear spin ensemble to demonstrate quantum interference phenomenon, i.e., an analog of EIT in an atomic ensemble coupled to light. This system is implemented by cantilevers tipped with ferromagnetic particles, producing inhomogeneous magnetic fields which couple the mechanical tips to the spin ensemble. We have studied the dynamical properties in this NAMR–spin ensemble–NAMR system by applying a probe microwave field. In the low-excitation approximation with the large-N limit, this NAMR–spin ensemble–NAMR coupling system behaves as a system of three coupled harmonic oscillators. As a result, there is a so-called double EIT effect in this system, with two absorption windows. Furthermore, we have shown that the group velocity of the microwave field is reduced dramatically in both of these two windows.

Finally, we point out that the NAMR–spin ensemble–NAMR coupling system is a subnetwork of a structure consisting of an array of NAMRs and nuclear spin ensembles, where the quantum information of the NAMR can be stored in the nuclear spin ensemble for a long time and transferred to the next NAMR at a distance. And this process is repeated in the next subnetworks. Therefore, it is expected that the spin ensembles can behave as a quantum transducer that stores and transfers the quantum information of the NAMRs.

ACKNOWLEDGMENTS

The work is supported by the National Natural Science Foundation of China under Grants No. 10935010 and No. 11074261.

[1] D. Bouwmeeste, A. Ekert, and A. Zeilinger, eds., *The Physics of Quantum Information* (Springer, Berlin, 2000).
[2] J. I. Cirac and P. Zoller, Phys. Rev. Lett. **74**, 4091 (1995).
[3] D. P. DiVincenzo and C. Bennet, Nature (London) **404**, 247 (2000).
[4] Y. Li, T. Shi, B. Chen, Z. Song, and C. P. Sun, Phys. Rev. A **71**, 022301 (2005).
[5] T. Shi, Y. Li, Z. Song, and C. P. Sun, Phys. Rev. A **71**, 032309 (2005).
[6] S. E. Harris, Phys. Today **50**(7), 36 (1997).
[7] L. V. Hau, S. E. Harris, Z. Dutton, and C. H. Behroozi, Nature (London) **397**, 594 (1999).
[8] M. M. Kash, V. A. Sautenkov, A. S. Zibrov, L. Hollberg, G. R. Welch, M. D. Lukin, Y. Rostovtsev, E. S. Fry, and M. O. Scully, Phys. Rev. Lett. **82**, 5229 (1999).
[9] M. D. Lukin, M. Fleischhauer, A. S. Zibrov, H. G. Robinson, V. L. Velichansky, L. Hollberg, and M. O. Scully, Phys. Rev. Lett. **79**, 2959 (1997).
[10] M. Fleischhauer and M. D. Lukin, Phys. Rev. Lett. **84**, 5094 (2000).
[11] D. F. Phillips, A. Fleischhauer, A. Mair, R. L. Walsworth, and M. D. Lukin, Phys. Rev. Lett. **86**, 783 (2001).
[12] C. Liu, Z. Dutton, C. H. Behroozi, and L. V. Hau, Nature (London) **409**, 490 (2001).
[13] C. P. Sun, Y. Li, and X. F. Liu, Phys. Rev. Lett. **91**, 147903 (2003).
[14] Y. Li and C. P. Sun, Phys. Rev. A **69**, 051802(R) (2004).
[15] Z. Song, P. Zhang, T. Shi, and C. P. Sun, Phys. Rev. B **71**, 205314 (2005).
[16] L. Zhou, Y. B. Gao, Z. Song, and C. P. Sun, Phys. Rev. A **77**, 013831 (2008).
[17] J. Q. Liao, J. F. Huang, Y.-X. Liu, L. M. Kuang, and C. P. Sun, Phys. Rev. A **80**, 014301 (2009).
[18] J. Q. Liao, Z. R. Gong, L. Zhou, Y.-X. Liu, C. P. Sun, and F. Nori, Phys. Rev. A **81**, 042304 (2010).
[19] J. M. Taylor, C. M. Marcus, and M. D. Lukin, Phys. Rev. Lett. **90**, 206803 (2003).
[20] M. H. Levitt, *Spin Dynamics: Basics of Nuclear Magnetic Resonance*, 2nd ed. (Wiley, New York, 2008).
[21] A. Imamoğlu, E. Knill, L. Tian, and P. Zoller, Phys. Rev. Lett. **91**, 017402 (2003).
[22] M. Poggio, G. M. Steeves, R. C. Myers, Y. Kato, A. C. Gossard, and D. D. Awschalom, Phys. Rev. Lett. **91**, 207602 (2003).
[23] M. Kroutvar, Y. Ducommun, D. Heiss, M. Bichler, D. Schuh, G. Abstreiter, and J. J. Finley, Nature (London) **432**, 81 (2004).
[24] S. Mancini and P. Tombesi, Phys. Rev. A **49**, 4055 (1994).
[25] S. Bose, K. Jacobs, and P. L. Knight, Phys. Rev. A **59**, 3204 (1999).
[26] W. Marshall, C. Simon, R. Penrose, and D. Bouwmeester, Phys. Rev. Lett. **91**, 130401 (2003).
[27] D. Vitali, S. Gigan, A. Ferreira, H. R. Böhm, P. Tombesi, A. Guerreiro, V. Vedral, A. Zeilinger, and M. Aspelmeyer, Phys. Rev. Lett. **98**, 030405 (2007).
[28] C. Genes, D. Vitali, and P. Tombesi, Phys. Rev. A **77**, 050307 (2008).
[29] H. Ian, Z. R. Gong, Y.-X. Liu, C. P. Sun, and F. Nori, Phys. Rev. A **78**, 013824 (2008).
[30] Y. Chang, H. Ian, and C. P. Sun, J. Phys. B **42**, 215502 (2009).
[31] S. Mancini, D. Vitali, and P. Tombesi, Phys. Rev. Lett. **80**, 688 (1998).
[32] M. Bhattacharya and P. Meystre, Phys. Rev. Lett. **99**, 073601 (2007).
[33] M. Bhattacharya, H. Uys, and P. Meystre, Phys. Rev. A **77**, 033819 (2008).
[34] C. Genes, D. Vitali, P. Tombesi, S. Gigan, and M. Aspelmeyer, Phys. Rev. A **77**, 033804 (2008).
[35] K. Hammerer, K. Stannigel, C. Genes, and P. Zoller, P. Treutlein, S. Camerer, D. Hunger, and T. W. Hänsch, Phys. Rev. A **82**, 021803(R) (2010).
[36] S. Bose, K. Jacobs, and P. L. Knight, Phys. Rev. A **56**, 4175 (1997).
[37] Z. R. Gong, H. Ian, Y.-X. Liu, C. P. Sun, and F. Nori, Phys. Rev. A **80**, 065801 (2009).
[38] M. Wallquist, K. Hammerer, P. Zoller, C. Genes, M. Ludwig, F. Marquardt, P. Treutlein, J. Ye, and H. J. Kimble, Phys. Rev. A **81**, 023816 (2010).
[39] K. C. Schwab and M. L. Roukes, Phys. Today **58**(7), 36 (2005).
[40] L. G. Remus, M. P. Blencowe, and Y. Tanaka, Phys. Rev. B **80**, 174103 (2009).
[41] D. Rugar, C. S. Yannoni, and J. A. Sidles, Nature (London) **360**, 563 (1992).
[42] J. A. Sidles, J. L. Garbini, K. J. Bruland, D. Rugar, O. Züger, S. Hoen, and C. S. Yannoni, Rev. Mod. Phys. **67**, 249 (1995).
[43] D. Rugar, R. Budakian, H. J. Mamin, and B. W. Chui, Nature (London) **430**, 329 (2004).
[44] R. Budakian, H. J. Mamin, B. W. Chui, and D. Rugar, Science **307**, 408 (2005).
[45] H. J. Mamin, M. Poggio, C. L. Degen, and D. Rugar, Nature Nanotechnol. **2**, 301 (2007).
[46] C. L. Degen, M. Poggio, H. J. Mamin, and D. Rugar, Phys. Rev. Lett. **99**, 250601 (2007).
[47] C. L. Degen, M. Poggio, H. J. Mamin, and D. Rugar, Phys. Rev. Lett. **100**, 137601 (2008).
[48] F. Xue, L. Zhong, Y. Li, and C. P. Sun, Phys. Rev. B **75**, 033407 (2007).
[49] M. Poggio, H. J. Mamin, C. L. Degen, M. H. Sherwood, and D. Rugar, Phys. Rev. Lett. **102**, 087604 (2009).
[50] P. C. Layterbur, Nature (London) **242**, 190 (1973).
[51] P. Rabl, S. J. Kolkowitz, F. H. L. Koppens, J. G. E. Harris, P. Zoller, and M. D. Lukin, Nature Phys. **6**, 602 (2010).
[52] C. P. Sun, L. F. Wei, Y.-X. Liu, and F. Nori, Phys. Rev. A **73**, 022318 (2006).
[53] M. O. Scully and M. S. Zubairy, *Quantum Optics* (Cambridge University Press, Cambridge, 1997).
[54] C. L. G. Alzar, M. A. G. Martinez, and P. Nussenzveig, Am. J. Phys. **70**, 37 (2002).
[55] J. D. Jackson, *Classical Electrodynamics*, 3rd ed. (Wiley, New York, 1999).
[56] M. N. Makhonin, E. A. Chekhovich, P. Senellart, A. Lemaître, M. S. Skolnick, and A. I. Tartakovskii, Phys. Rev. B **82**, 161309(R) (2010).